Bioresources and Bioprocessing

RESEARCH

Open Access

Effect of temperature and surfactant on biomass growth and higher-alcohol production during syngas fermentation by *Clostridium carboxidivorans* P7

Shaohuang Shen[1], Guan Wang[1], Ming Zhang[1], Yin Tang[1], Yang Gu[2], Weihong Jiang[2], Yonghong Wang[1*] and Yingping Zhuang[1*]

Abstract

Hexanol–butanol–ethanol fermentation from syngas by *Clostridium carboxidivorans* P7 is a promising route for biofuel production. However, bacterial agglomeration in the culture of 37 °C severely hampers the accumulation of biomass and products. To investigate the effect of culture temperature on biomass growth and higher-alcohol production, *C. carboxidivorans* P7 was cultivated at both constant and two-step temperatures in the range from 25 to 37 °C. Meanwhile, Tween-80 and saponin were screened out from eight surfactants to alleviate agglomeration at 37 °C. The results showed that enhanced higher-alcohol production was contributed mainly by the application of two-step temperature culture rather than the addition of anti-agglomeration surfactants. Furthermore, comparative transcriptome revealed that although 37 °C promoted high expression of genes involved in the Wood–Ljungdahl pathway, genes encoding enzymes catalyzing acyl-condensation reactions associated with higher-alcohol production were highly expressed at 25 °C. This study gained greater insight into temperature-effect mechanism on syngas fermentation by *C. carboxidivorans* P7.

Keywords: *Clostridium carboxidivorans* P7, Higher alcohol, Two-step temperature culture, Surfactant, Comparative transcriptome

Introduction

Biofuel production is developed as a sustainable alternative to deal with the global demand of energy due to diminishing fossil fuel reserves and increasing greenhouse gases generated from using fossil fuels (Latif et al. 2014). As one of emerging production approaches, syngas fermentation utilizes acetogens to fix carbon-containing gas to biofuel, which accommodates numerous sources of raw materials, including industrial, agricultural and municipal wastes (Ramachandriya et al. 2013). A wide range of carbon-containing materials can be first converted into syngas which can indistinguishably be used by gas-fermenting microbes. Besides, some CO-rich industrial waste gases, e.g., waste gas from steel industries can be directly fermented (Latif et al. 2014; Molino et al. 2018).

Clostridium carboxidivorans P7 is one of model organisms widely studied for hexanol–butanol–ethanol fermentation from syngas, it employs the Wood–Ljungdahl pathway (WL pathway) to convert CO or CO_2 into acetyl-CoA, and finally produces two–six carbon chain (C2–C6) alcohols and acids (Fernández-Naveira et al. 2017b). In comparison with ethanol, higher-alcohols (designated as butanol and hexanol in this study) have featured with superb fuel characteristics more than higher energy

*Correspondence: yhwang@ecust.edu.cn; ypzhuang@ecust.edu.cn
[1] State Key Laboratory of Bioreactor Engineering, East China University of Science and Technology, Shanghai 200237, China
Full list of author information is available at the end of the article

contents. For example, butanol is more suitable for use as its less explosive, less hygroscopic, less volatile and less corrosive than ethanol (Lee et al. 2008). Besides, it can be used in pure form or blended at any concentration with gasoline in combustion engines (Dürre 2007). Likewise, hexanol has many industrial applications owing to its hypotoxicity at low concentrations for use in cosmetic, textile and pharmaceutical industries (Fernández-Naveira et al. 2017b). In addition, hexanol is considered for blending with diesel as an aviation fuel (Fernández-Naveira et al. 2017b; Yeung and Thomson 2013).

However, higher-alcohol production from syngas has long been far from reach on large-scale. There are some challenges imperiling its economic competitiveness, such as low higher-alcohol production and low culture density. On one hand, low higher-alcohol production is caused by low biomass concentration. In the published studies, the cellular optical densities at 600 nm or 660 nm (OD_{600}s or OD_{660}s) of *C. carboxidivorans* P7 were generally around 1.0 (approx. biomass concentration of 0.3 g/l) (Fernández-Naveira et al. 2016, 2019; Phillips et al. 2015; Ramió-Pujol et al. 2015a). Even, bacterial agglomeration during syngas fermentation was observed, which significantly limited the biomass growth (Shen et al. 2017). Furthermore, the growth of this strain is inhibited by end-products (Zhang et al. 2016). Because alcohols have a cytotoxicity of disrupting the membrane structure and affecting its functions (Inoue and Horikoshi 1989), even at a very low concentration of 0.1% (v/v) (Sardessai and Bhosle 2002). On the other hand, the concentration ratios of higher-alcohols in total products are usually low. The distribution of products was found to be largely dependent on the growth conditions, e.g., culture temperature and trace metals composition, but the mechanism has remained unclear (Phillips et al. 2015; Ramió-Pujol et al. 2015a; Shen et al. 2017).

In our previous study, bacterial agglomeration by *C. carboxidivorans* P7 resulting in low higher-alcohol titer during syngas fermentation was found in the constant temperature culture (CT culture) of 37 °C; unexpectedly, the agglomeration was addressed by using a two-step temperature culture (TST culture), and butanol and hexanol were subsequently observed at considerable concentrations (Shen et al. 2017). However, it was unclear whether bacterial agglomeration or temperature mainly affected higher-alcohol production as different temperature settings were adopted in two cases. Therefore, more fermentation profiles using different temperature strategies including CT culture and TST culture were supplemented to systematically estimate the effect of temperature on syngas fermentation by *C. carboxidivorans* P7. The effective surfactants, which eliminated the interference of bacterial agglomeration at 37 °C were screened out and added into the medium to further determine the role of temperature on higher-alcohol production. Finally, comparative transcriptomic analysis was performed to investigate the temperature-effect mechanism at a molecular level.

Materials and methods

Strains and culture conditions

C. carboxidivorans P7 (DSM-15243) used in this study was obtained from the DSMZ culture collection. This strain was stored in 10% (v/v) glycerol at − 80 °C, revived in Wilkins Chalgren anaerobe broth (WCB), and cultured in a strict anaerobic environment at 37 °C (Shen et al. 2017).

Bottle fermentation

Both the seed culture and the formal fermentation were carried out using 125-ml serum bottles (Sigma, St. Louis, MO, USA) loading with 30 ml optimized ATCC 1754 medium (Shen et al. 2017). Primary culture (the OD_{600} of approx. 1.5 in WCB) was inoculated into a serum bottle with 5% (v/v) inoculum size, and the headspace of the bottle was filled with the model syngas ($CO:CO_2:H_2:Ar = 56:20:9:15$) at an overpressure of 0.2 MPa. The sealed bottle was fixed in the shaker at 100 rpm and incubated at 37 °C. After 24 h, 5% (v/v) culture from the above seed bottle was inoculated into the prepared serum bottles loading with fresh medium for formal fermentation experiments. The bottles for formal fermentation experiments were done as the seed bottle, but incubated at the required temperature and refreshed the syngas every 24 h. All the bottle fermentation experiments were carried out in triplicate and replicated in a timely manner.

The supplementary details of experiments are as follows:

CT culture experiment: four groups of inoculated bottles were, respectively, incubated at 25 °C, 29 °C, 33 °C and 37 °C for 120 h.

TST culture experiment: in the first 24 h, three groups of inoculated bottles were incubated at 37 °C and then, respectively, transferred to 25 °C, 29 °C and 33 °C for further 96 h till to a total of 120 h. A control group was kept at 37 °C for 120 h.

TST culture experiment combined with surfactant addition: a group of inoculated bottles with 0.1% (w/w) Tween 80 in the broth and other one with 0.1% (w/w) saponin were cultured at 37 °C for 120 h as well as a control group without any surfactant; another three groups prepared the same as above were cultured at 37 °C for the first 24 h and transferred to 25 °C for further 96 h till a total of 120 h.

Growth and biomass measurement

300 µl of sample was daily removed from the experimental bottle for growth measurement in the process of syngas fermentation, by OD_{600} on a visible light spectrophotometer (722S, Shanghai Precision, Shanghai, China). Biomass concentration (g/l) was directly weighed using dried cell at the end of fermentation time.

Biomass-carbon content measurement

The carbon content of the biomass was determined as $47.05 \pm 0.80\%$ (w/w) using an elemental analyzer (Vario EL III, Elementar Analysen systeme GmbH, Hanau, Germany).

Bottle off-gas measurement

Bottle off-gas was collected using a 100-ml gas collection bag before the gas was refreshed every day, and then measured by a gas mass spectrometer (MAX300-LG, Extrel, Pittsburgh, PA, USA).

Fermentation product measurement

300 µl of sample was removed from the experimental bottle at the end of fermentation time for detection of acids (acetate, butyrate and caproate) and alcohols (ethanol, butanol and hexanol) using gas chromatography (7890 A, Agilent, Wilmington, DE, USA) as described previously (Shen et al. 2017).

Transcriptional response in different temperature culture

RNA isolation, cDNA library preparation and transcriptome sequencing

Two time-point samples were, respectively, collected in the early and late stages of the culture pattern of 37 °C, 25 °C and 37–25 °C. The choice of sampling time took the difference of the physiological stage of this strain under three culture conditions into account. A total of five time-point samples in triplicate were collected: C37-24 (24 h in the CT culture of 37 °C/TST culture of 37–25 °C), C37-48 (48 h in the CT culture of 37 °C), C25-72 (72 h in the CT culture of 25 °C), C25-120 (120 h in the CT culture of 25 °C) and T-72 (72 h in the TST culture of 37–25 °C). Total RNA was isolated and purified according to the method described as the protocol of RNA extraction kit (Axygen Scientific, Inc., USA). The quantity of RNA was evaluated using the NanoPhotometer spectrophotometer (Implen, CA, USA) and required with the A260/A280 and A260/230 of no less than 2.0 and 1.5, respectively; the integrity of RNA was evaluated using the Bioanalyzer 2100 (Agilent, Santa Clara, USA) and required with the RIN of no less than 7.0. The qualified samples were used for mRNA-seq library construction after deleting rRNA using rRNA removal kit (Illumina, San Diego, CA, USA). RNA-seq transcriptome library was sequenced on the Illumina sequencing platform (GeneDenovo, Guangzhou, China).

Bioinformation analysis

Raw data were filtered to clean reads of high quality after trimming some invalid and redundant data, and then removed reads mapped to RNA ribosome using Bowtie 2. Retained reads were aligned with the reference genome to identify known genes and calculated gene expression by RSEM (Li and Dewey 2011). The gene expression was further normalized using the fragments per kilobase of transcript per million mapped reads (FPKMs). Differentially expressed genes (DEGs) were identified as those with the false discovery rate (FDR) of less than 0.05 and the absolute value of log2 fold change (log2FC) of not less than 1 using edgeR (https://www.r-project.org/). DEGs were then subjected to an enrichment analysis of KEGG pathways, and FDRs were corrected using less than 0.05 as threshold. FPKMs of putative encoding genes of each enzyme/enzyme involved in the WL pathway and C2–C6 product biosynthetic pathway were normalized in a heat map to estimate relative expression level based on OmicShare, an online platform for data analysis (https://www.omicsmart.com/).

Results and discussion

Effect of CT culture on growth and production

As shown in Fig. 1a, the growth of *C. carboxidivorans* P7 was observed in the range from 25 to 37 °C, which fully confirmed that *C. carboxidivorans* P7 had a good adaptability to temperature (Fernández-Naveira et al. 2017a; Latif et al. 2014). The growth curves of the bacteria at 33 °C and 37 °C were almost identical and after 48 h, the OD_{600}s at both 33 °C and 37 °C decreased as the bacteria agglomerated. Even though the flocculated agglomerates were not observed at 25 °C and 29 °C, the growth rates were much lower than those at 37 °C and 33 °C. At the end of 120 h fermentation, the biomass concentrations at 33 °C and 37 °C were both approximately 0.60 g/l, significantly higher than about 0.20 g/l at 25 °C and 29 °C. Within a certain range, higher temperature shortens the lag period and stimulates cell growth, which is a well-accepted nature for microbial metabolism (Price and Sowers 2004).

As shown in Fig. 1b, the maximum titers of ethanol and acetate were, respectively, 3.43 ± 0.08 g/l and 0.93 ± 0.12 g/l, occurring at 37 °C, while the minimum titers were, respectively, 1.58 ± 0.03 g/l and 0.61 ± 0.15 g/l, appearing at 25 °C. Ethanol and acetate are both growth-related products (Fernández-Naveira

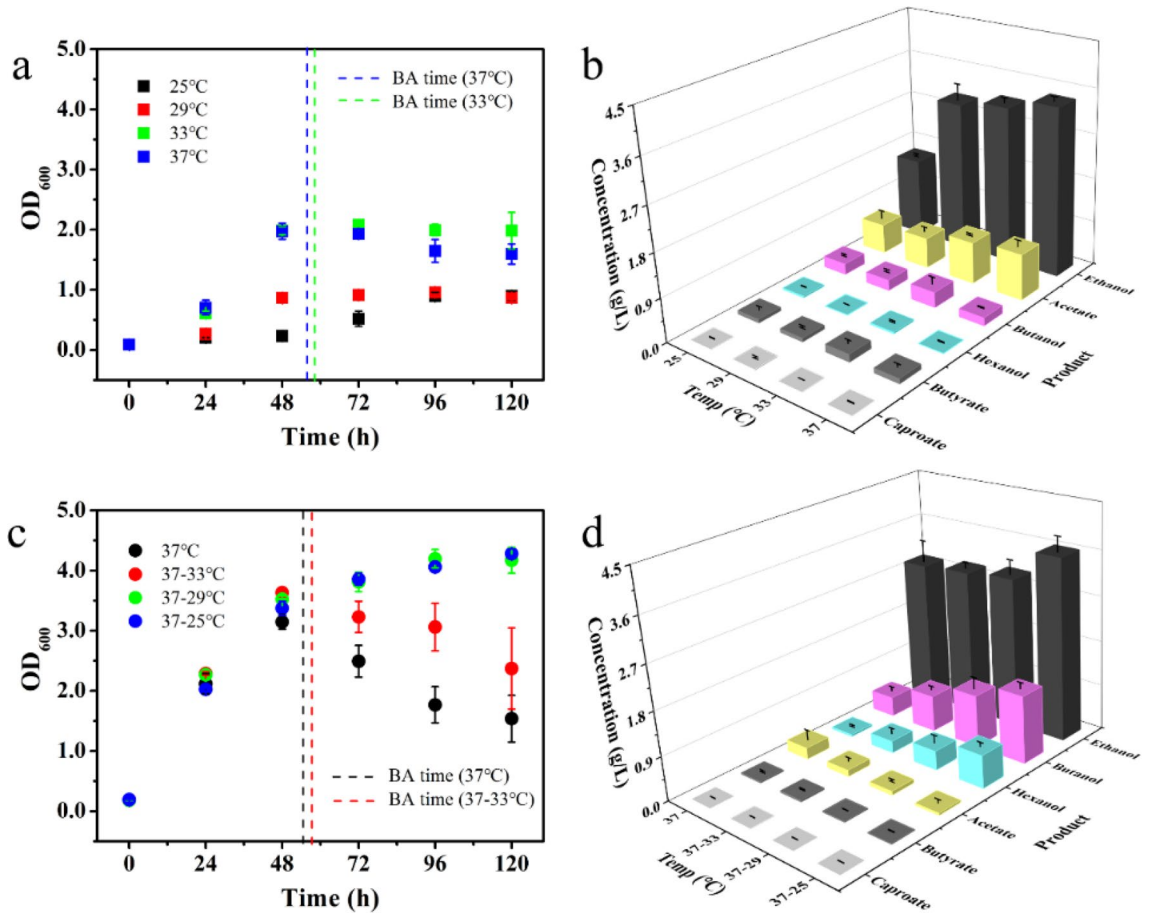

Fig. 1 Growth and production by *C. carboxidivorans* P7 using various temperature strategies. Mean values and standard errors of three replicates are shown in all graphs. **a** Optical densities at 600 nm (OD_{600}s) in the culture of 25 °C, 29 °C, 33 °C and 37 °C, respectively, during 0–120 h; the approximate time when bacterial agglomerates appeared (BA time) in the culture of 33 °C and 37 °C. **c** OD_{600}s in the culture of 37–25 °C, 37–29 °C, 37–33 °C and 37 °C, respectively, during 0–120 h; the BA time in the culture of 37 °C and 37–33 °C. **b**, **d** Titers of ethanol, butanol, hexanol, acetate, butyrate and caproate at 120 h, using various temperature strategies

et al. 2019; Shen et al. 2017), their production preferred 37 °C to 25 °C. Interestingly, although acetate titers among the experimental groups were low (< 1.0 g/l) using the previous modified medium (Shen et al. 2017) in this study, it still showed a weakening trend with the decreasing temperature, verifying that low temperature facilitated organic acid re-assimilation (Ramió-Pujol et al. 2015a; Shen et al. 2017). By contrast, the minimum titer of butanol was 0.16 ± 0.01 g/l at 37 °C. As shown in Table 1, the special production rate (SPR) of butanol increased substantially as the temperature decreased and the maximum was 0.20 ± 0.02 g/(day g biomass) at 25 °C, suggesting that the production potential of butanol was motivated at low temperature (Ramió-Pujol et al. 2015a; Shen et al. 2017; Zhang et al. 2016). Similar to acetate, butyrate titer reached above 0.1 g/l at 33 °C and 37 °C while only trace amounts were observed at 25 °C and 29 °C.

In the late culture stage of 37 °C, there were macroscopic agglomerates in the bottle (Fig. 2a). The agglomerated cells stained with methylthionine chloride were observed composed of bacterial communities wrapped in extracellular polymeric substance (EPS) under the microscope (Fig. 2b). Bacterial EPS generally consisted of polysaccharides, proteins, and nucleic acids secreted by cells (Nielsen and Jahn 1999; Sheng et al. 2010). It contributes to the key structure of biofilms in order to enhance resistance to harsh environments (Sheng et al. 2010), commonly found in *Clostridium* species (Pantaléon et al. 2014). Conversely, there was homogeneous fermentation broth without bacterial agglomerates in the bottle and bacteria without EPS under the microscope in the late culture stage of 25 °C (Fig. 2c, d).

Table 1 The specific production rates of various alcohols by *C. carboxidivorans* P7 using different culture strategies

Growth conditions	Alcohol specific production rate[a] (g alcohol/(day g biomass))		
	Ethanol	Butanol	Hexanol
25 °C	1.38 ± 0.09	0.20 ± 0.02	0.03 ± 0.01
29 °C	2.46 ± 0.18	0.18 ± 0.02	0.01 ± 0.00
33 °C	0.99 ± 0.04	0.10 ± 0.04	0.01 ± 0.01
37 °C	1.14 ± 0.04	0.05 ± 0.00	0.00 ± 0.00
37 °C	0.71 ± 0.13	0.10 ± 0.01	0.01 ± 0.00
37–33 °C	0.62 ± 0.02	0.16 ± 0.01	0.05 ± 0.02
37–29 °C	0.55 ± 0.03	0.19 ± 0.04	0.07 ± 0.03
37–25 °C	0.66 ± 0.04	0.25 ± 0.01	0.12 ± 0.01
Control-37 °C	0.72 ± 0.06	0.04 ± 0.00	0.00 ± 0.00
Control-37–25 °C	0.53 ± 0.00	0.23 ± 0.00	0.15 ± 0.01
Tween 80-37 °C	1.17 ± 0.18	0.13 ± 0.03	0.02 ± 0.01
Tween 80-37–25 °C	0.67 ± 0.08	0.23 ± 0.02	0.10 ± 0.01
Saponin-37 °C	0.50 ± 0.00	0.09 ± 0.00	0.01 ± 0.00
Saponin-37–25 °C	0.62 ± 0.10	0.16 ± 0.02	0.05 ± 0.01

[a] Mean values and standard errors of three replicates are shown

Effect of TST culture on growth and production

The application of the TST culture proved to be an effective solution to balance biomass growth and alcohol production, which was not the case in the CT culture, e.g., bacterial agglomeration (Shen et al. 2017). To systematically evaluate temperature combination in the TST culture, three temperature gradients (37–33 °C, 37–29 °C and 37–25 °C) were carried out in syngas fermentation by *C. carboxidivorans* P7.

When the temperature was down-regulated to 33 °C in the second-stage culture (24–120 h), the bacteria were observed to agglomerate during 48–72 h as the control in the CT culture of 37 °C (Fig. 1c), which additionally indicated that there were no obvious differences between incubation at 33 °C and 37 °C for the growth of this strain. However, when adopting 29 °C or 25 °C in the second-stage culture, bacterial agglomeration was not observed through the whole fermentation process, and the growth rates only slightly declined after the temperature switched (Fig. 1c). At 120 h, compared to the control, the biomass concentrations increased by 55.77% and 54.57% in the TST culture of 37–29 °C and 37–25 °C, respectively. These results illustrated both the TST culture of 37–29 °C and 37–25 °C could improve culture density, which was limited by agglomeration at 37 °C.

Furthermore, all alcohol titers increased as the temperature decreased in the second-stage culture (Fig. 1d). The maximum titers of ethanol, butanol and hexanol, 3.64 ± 0.29 g/l, 1.35 ± 0.10 g/l and 0.66 ± 0.06 g/l, respectively, all occurred at 37–25 °C (Fig. 1d). On one hand, the enhanced alcohol production benefited from the promoting culture density. On the other hand, it should be emphasized that the greater production potentials of hexanol and butanol were exploited in high-density culture at low temperature. Referring to the SPRs (Table 1), the SPR of butanol at 37–25 °C increased slightly to 0.25 ± 0.01 g/(day g biomass) from 0.20 ± 0.02 g/(day g biomass) at 25 °C, and that of hexanol had a great improvement, up to 0.12 ± 0.01 g/(day g biomass), compared to 0.03 ± 0.01 g/(day g biomass) at 25 °C. Meanwhile, acetate titer declined with the decreasing temperature in the second-stage culture, from 0.23 ± 0.18 g/l at 37 °C to 0.05 ± 0.05 g/l at 37–25 °C, confirming low temperature controlled in the second-stage culture could also facilitate organic acid re-assimilation. Similar to the fermentation broth at 25 °C, there was homogeneous fermentation broth and cells without EPS in the late culture stage of 37–25 °C.

These data demonstrated that the superiority of the TST culture with higher alcohol production as well as higher culture density than the CT culture. Maddox et al. (2000) also used a TST culture in acetone–butanol–ethanol fermentation by *Clostridium beijerinckii*. The difference was their fermentation started at 28 °C and the temperature was increased to 34 °C during solventogenesis. This operation was designed to reduce growth rate in exponential phase to minimize acetate accumulation and accelerate alcohol production during solventogenesis, finally leading to improved fermentation efficiency. However, this study adopted 37 °C in the first 24 h of fermentation, aiming at accumulating high density of bacteria in a short time and subsequently down-regulated temperature to induce the bacteria to produce more higher-alcohols.

Effect of TST culture combined with surfactant addition on growth and production

The use of surfactants has been reported to disperse microbial agglomerates as biofilm (Felmann et al. 1974). In the screening experiment of eight surfactants, it was found that 0.1% (w/w) saponin or Tween 80 in the broth could effectively alleviate bacterial agglomeration in the CT culture of 37 °C (Additional file 1: Fig. S1). Hence, we further verified the role of temperature on syngas fermentation based on anti-agglomerating action from saponin or Tween 80.

In the CT culture of 37 °C, the addition of Tween 80 or saponin significantly promoted the bacterial growth compared to the control at 37 °C, even the saponin-adding group reached a high density of OD_{600} 4.0; while adopting the TST culture of 37–25 °C combined with the addition of Tween 80 or saponin, the growth was not

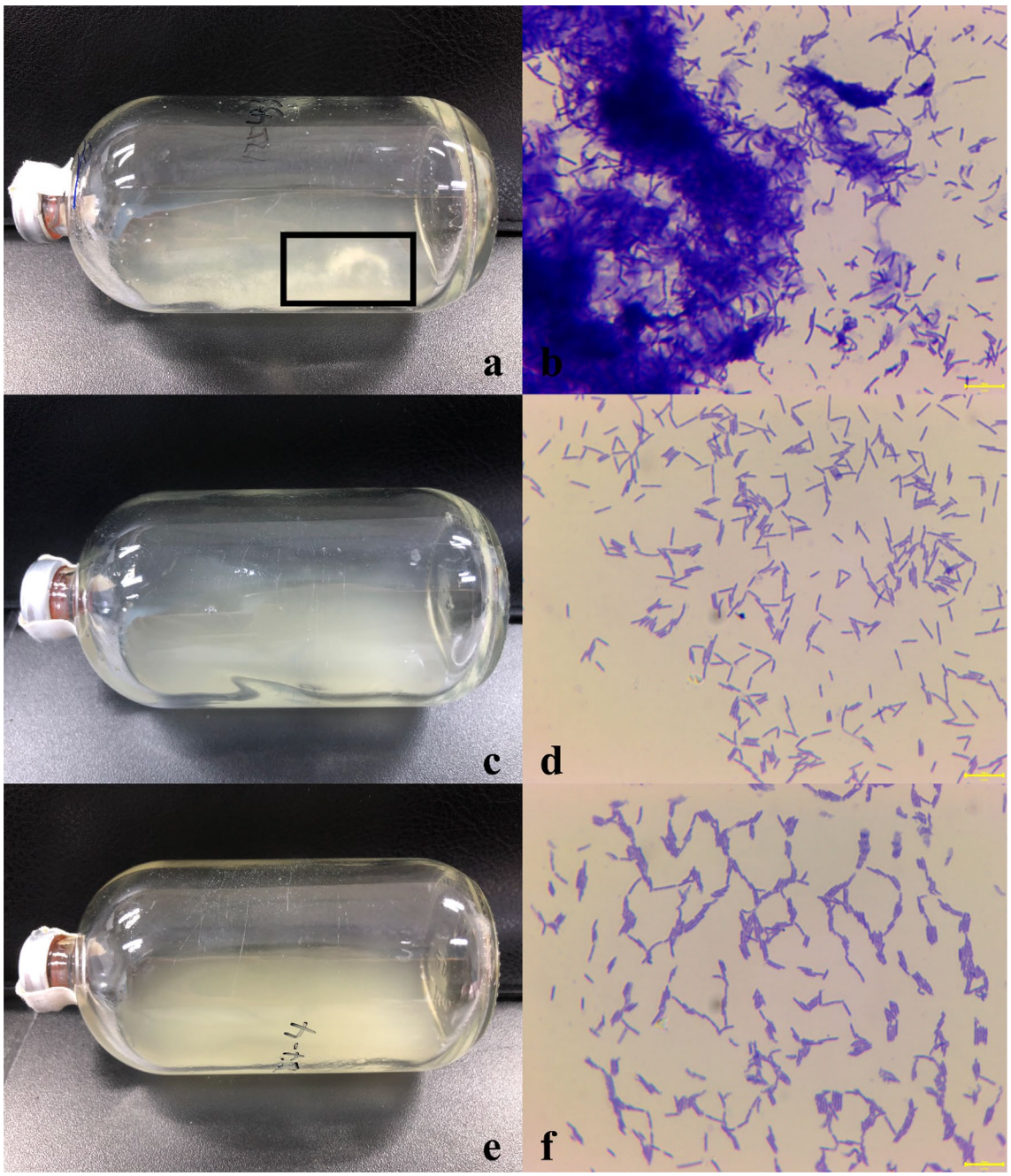

Fig. 2 The morphologic pictures of *C. carboxidivorans* P7 in serum bottle and under the microscope using various temperature strategies. The broth in serum bottle in the late culture stage of **a** 37 °C, **c** 25 °C and **e** 37–25 °C, respectively. The microscopic examination of the corresponding broth in the late culture stage of **b** 37 °C, **d** 25 °C and **f** 37–25 °C, respectively, using methylene blue staining (1000×)

further improved compared to the control at 37–25 °C (Fig. 3a–c), implied the positive effect from the surfactants worked on the bacteria only at 37 °C.

Substrate consumption clearly demonstrated the effect of the two strategies. In the control at 37 °C, CO content in off-gas only decreased by 11.96 ± 4.44% during 48–72 h and was unchanged after 72 h, consistent with the appearance time of bacterial agglomerates (Table 2). The bacterial agglomerates aggravated gas–liquid transfer limitation, which is originally considered a major bottleneck in syngas fermentation (Latif et al. 2014; Wainaina et al. 2018). At 37 °C, the addition of Tween 80

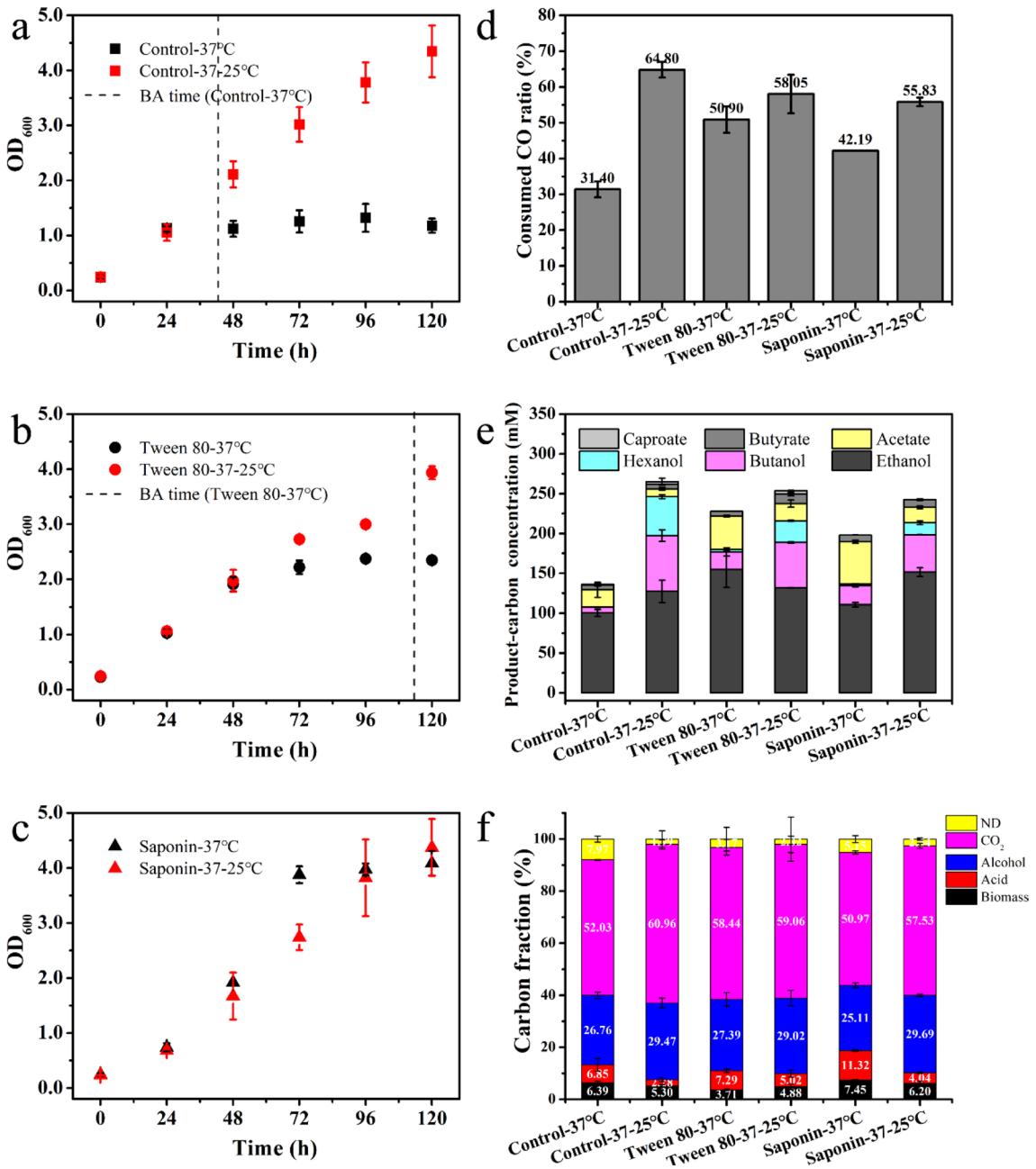

Fig. 3 Growth, production, carbon monoxide consumption and carbon fraction by *C. carboxidivorans* P7 using different culture strategies. Mean values and standard errors of three replicates are shown in all graphs. Optical densities at 600 nm (OD_{600}s) in the culture of 37 °C and 37–25 °C, **a** without any surfactant, **b** with Tween 80 and **c** with saponin; and **a**, **b** the approximate time when bacterial agglomerates appeared (the BA time) in the culture of 37 °C. **d** Consumed carbon monoxide ratios during 0–120 h. **e** Product-carbon concentrations (mmol/l) from ethanol, butanol, hexanol, acetate, butyrate and caproate at 120 h. **f** Carbon fraction at 120 h, mainly consisting of biomass, alcohol, acid, carbon dioxide and not detected unknown

or saponin into culture enhanced the resistance to bacterial agglomeration so that the CO intake by *C. carboxidivorans* P7 continued until least 96 h (Table 2). Compared to the control at 37 °C without any surfactants, the consumed CO ratios increased by 19.50% and 10.79%, respectively (Fig. 3d); meanwhile, product-carbon concentrations increased by 91.59 mmol/l and 61.75 mmol/l, respectively (Fig. 3e).

In the TST culture of 37–25 °C, CO consumption in three experimental groups continued throughout

Table 2 The consumed carbon monoxide ratios during fermentation process by *C. carboxidivorans* P7 using different culture strategies

Growth conditions	Consumed CO ratio[a,b] (%)				
	0–24 h	24–48 h	48–72 h	72–96 h	96–120 h
Control-37 °C	54.87 ± 6.43	90.18 ± 1.51	11.96 ± 4.44	ND[c]	ND[c]
Control-37–25 °C	49.85 ± 2.64	73.61 ± 16.03	68.88 ± 10.87	86.89 ± 0.77	44.88 ± 19.33
Tween 80-37 °C	47.06 ± 5.93	88.06 ± 4.83	73.30 ± 11.42	39.06 ± 19.00	6.99 ± 9.88
Tween 80-37–25 °C	50.55 ± 3.18	73.30 ± 7.47	53.89 ± 15.37	79.59 ± 5.82	32.85 ± 4.94
Saponin-37 °C	26.87 ± 2.86	85.26 ± 1.76	85.03 ± 1.43	13.82 ± 0.00	ND[c]
Saponin-37–25 °C	28.16 ± 4.22	72.16 ± 18.95	77.70 ± 6.40	85.37 ± 3.23	15.79 ± 27.35

[a] Mean values and standard errors of three replicates are shown

[b] The ratio of the consumed to the renew of CO every 24 h

[c] ND represents the CO consumption was not detected

the whole fermentation time of 120 h (Table 2), clearly suggesting that the TST culture of 37–25 °C had an advantage over the addition of surfactants at 37 °C on lengthening effective fermentation time. Furthermore, consumed CO ratio in the control at 37–25 °C was up to 64.80 ± 2.18%, slightly higher than those in the surfactant-adding groups at 37–25 °C (Fig. 3d), similar to the case for the product-carbon concentrations (Fig. 3e). These small differences between the control and the surfactant-adding groups indicated that the two surfactants added into the broth slightly inhibited carbon fixing and anabolism of the bacteria in reality, which was merely covered by severe bacterial agglomeration in the CT culture of 37 °C.

As reported, the presence of surfactant could release bacterial EPS by disturbing the binding interaction within and between EPS, and then destroy its conformation and function (Guan et al. 2017). In this study, Tween 80 and saponin were presumed based on this dispersive action to prevent bacteria from generating EPS for agglomeration, and thus led to homogeneous broth for mass transfer that benefited biomass growth and product production. Besides, saponin itself has been also reported to enhance growth of other bacteria, e.g., *Selenomonas ruminantium* (Wang et al. 2000). Sen et al. (1998) proposed that saponin at low concentrations could lead to a slight increase in cellular permeability, causing enhancement of nutrient transport and thus promoting growth. This explanation was based on the amphiphilic characteristics of surfactants. When the cellular permeability improved by surfactants exceeded the membrane tolerance, it would damage membrane structure and conversely inhibit cell viability. Therefore, in the presence of EPS at 37 °C, the surfactants promoted the growth, and in the absence of EPS at 37–25 °C, the surfactants inhibited cell metabolism.

In the CT culture of 37 °C, the addition of Tween 80 and saponin significantly got enhanced the SPRs of butanol, up to 0.13 ± 0.03 and 0.09 ± 0.00 g/(day g biomass), respectively, compared to the control group (37 °C) of 0.04 ± 0.00 g/(day g biomass); after using the TST culture of 37–25 °C combined with surfactant addition, these were further improved to 0.23 ± 0.02 and 0.16 ± 0.02 g/(day g biomass), respectively, but showed no superiority over the control (0.23 ± 0.00 g/(day g biomass) at 37–25 °C) (Table 1). Unexpectedly, the addition of surfactants did not work on hexanol production. Only after adopting the 37–25 °C strategy, the SPRs of hexanol were significantly improved, reaching 0.10 ± 0.01 and 0.05 ± 0.01 g/(day g biomass) in Tween 80-and saponin-adding group, respectively, and the control group also reached a higher value of 0.15 ± 0.01 g/(day g biomass). Compared to hexanol, butanol production was more likely to benefit from high-density culture, whether which was caused by the addition of surfactants or the application of TST culture. However, hexanol production seemed to be dependent on high-density culture at low temperature. The longer carbon chain was produced in the later fermentation time according to the chronological order with increased number of carbon atoms and increasing reducing equivalents (Ramachandriya et al. 2013). Low temperature adjusted in the late culture stage extended more effective fermentation time and may thus enhance hexanol production. From these data, a conclusion was drawn that low temperature played a more critical role in higher-alcohol production than anti-agglomeration.

In addition, this study conducted the experiments with a modal gas mixture of CO, CO_2, H_2 and Ar at a ratio of 56:20:9:15, which simulated the composition of off-gas from steel industry (Ar replaced N_2 for higher detection accuracy). In all experimental processes, only CO concentrations were detected in decrease, whereas CO_2

concentrations in net increase, and H_2 concentrations were almost unchanged. Presumably, hydrogenase was inhibited severely by CO at 11 μM (Drake 1982), and the lowest CO concentration in the broth calculated during syngas fermentation was approximately 156 μM. Therefore, CO was the main carbon and energy source consumed in this study. Younesi et al. (2005) also found that the consumption of H_2 and CO_2 was detected only after CO was exhausted in syngas fermentation by *Clostridium ljungdahlii*. Furthermore, after CO was assimilated by the bacteria, more than 50% carbon was lost in the form of CO_2 due to requirement of balancing reducing equivalents, more than 30% carbon flowed to products, and less than 10% of carbon was utilized for biomass building (Fig. 3f).

Temperature-effect mechanism revealed by comparative transcriptome analysis

Identification of DEGs

To analyze the transcriptional responses of *C. carboxidivorans* P7 under three culture patterns of 37 °C, 25 °C and 37–25 °C, two time-point samples were, respectively, collected in the early and late stages under each culture condition. RNA-seq quantitation data were obtained from five time-point samples (C37-24, C37-48, C25-72, C25-120 and T-72) in triplicate. Individual sample had an average of 22.8 million clean reads with an average of 99.55% mapping ratio (Additional file 2: Table S1). Therein, the number of all known genes reached to 5023, in contrast to 5079 reference genes of *C. carboxidivorans* P7, indicating these transcripts covered the expression of mostly genes of the reference genome. DEGs between the early and late stages under each culture condition were identified. There were 2664 DEGs (2338 up- and 326 down-regulated), 219 DEGs (101 up- and 118 down-regulated) and 1801 DEGs (1124 up- and 677 down-regulated) in the culture pattern of 37 °C, 25 °C and 37–25 °C, respectively.

KEGG pathway enrichment analysis of DEGs

These three groups of DEGs, which had 696, 88 and 585 candidate genes with pathway annotation in the culture pattern of 37 °C, 25 °C and 37–25 °C, respectively, were performed for KEGG pathway enrichment analysis (Additional file 2: Table S2) and the significantly enriched pathways ($P < 0.05$) are shown in Fig. 4.

As shown in Fig. 4a, the DEGs of C37-24-vs-C37-48 were significantly enriched in pentose and glucuronate interconversions (ko00040), glyoxylate and dicarboxylate metabolism (ko00630), ascorbate and aldarate metabolism (ko00053), and amino sugar and nucleotide sugar metabolism (ko00520), which belonged to carbohydrate

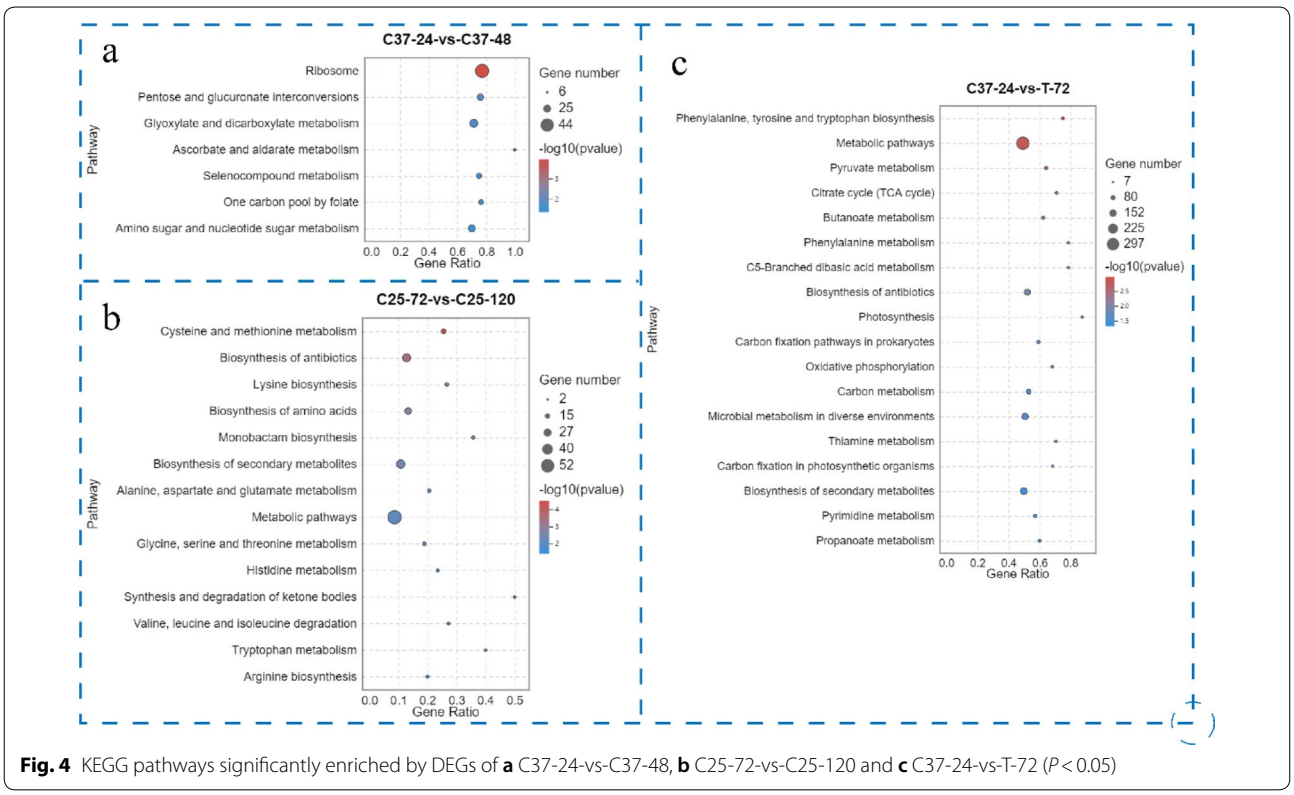

Fig. 4 KEGG pathways significantly enriched by DEGs of **a** C37-24-vs-C37-48, **b** C25-72-vs-C25-120 and **c** C37-24-vs-T-72 ($P < 0.05$)

metabolism, and most genes enriched in them were up-regulated in the late stage. This was likely related to the generation of EPS. Moreover, 41 out of 44 genes enriched in ribosome (ko03010) were down-regulated, suggesting agglomerated cells decreased translation level. Additionally, enriched selenocompound metabolism (ko00450) and one-carbon pool by folate (ko00670) indicated metabolism of other amino acids and metabolism of cofactors and vitamins played important roles in the process.

Interestingly, eight out of 14 enriched pathways by DEGs of C25-72-vs-C25-120 were related to amino acid metabolism such as cysteine and methionine metabolism (ko00270) and valine, leucine, isoleucine degradation (ko00280) (Fig. 4b), which may perform a special function for no EPS generation. In *Pseudomonas aeruginosa*, the inhibition of many reactions associated with fatty acid biosynthesis, arginine and proline metabolism, cysteine and methionine metabolism, valine, leucine, isoleucine degradation and butanoate metabolism was predicted to decrease biofilm formation (Vital-Lopez et al. 2015).

The DGEs of C37-24-vs-T-72 were enriched significantly in 18 pathways (Fig. 4c). In these pathways, five belonged to global and overview maps, five were related to carbohydrate metabolism, four were involved in energy metabolism, two were concerned with amino acid metabolism and the last two belonged to metabolism of cofactors and vitamins and nucleotide metabolism, respectively. The bacteria responded to temperature drop from 37 to 25 °C in the TST culture by regulating these pathways. Therein, there was a general up-regulated trend of DEGs (up-/down-DEGs > 1.5) in some enriched pathways involved in carbohydrate metabolism (ko00020: citrate cycle; ko00650: butanoate metabolism), energy metabolism (ko00195: photosynthesis; ko00720: carbon-fixation pathways in prokaryotes; ko00190: oxidative phosphorylation), amino acid metabolism (ko00360: phenylalanine metabolism) and metabolism of cofactors and vitamins (ko00730: thiamine metabolism).

That *C. carboxidivorans* P7 regulated transcriptional responses at different culture temperatures was a very complex process. Carbohydrate metabolism, energy metabolism and amino acid metabolism were mainly involved in this process. These significantly enriched pathways could help us to gain insight into temperature-relevant effects.

Expression of genes related to the WL pathway and C2–C6 product biosynthetic pathway

The WL pathway is a carbon-fixation pathway in *C. carboxidivorans* P7, divided into two branches: the methyl branch and the carbonyl branch (Fernández-Naveira et al. 2017b; Latif et al. 2014). These two branches provide one-carbon molecules that contribute to the formation of acetyl-CoA, which can then be assimilated into cellular biomass or converted to products. The biosynthetic pathway of C2–C4 products (ethanol, acetate, butanol and butyrate) has been illuminated in many literatures (Dürre 2007; Fernández-Naveira et al. 2017b). Although the native biosynthetic pathway of C6 products (hexanol and caproate) has not been defined so far, it is believed that carboxydotrophs synthesize C6 products via the CoA-dependent *Clostridium* pathway (Fernández-Naveira et al. 2017b; Ramió-Pujol et al. 2015b). Based on gene annotations from KEGG database, the WL pathway and C2–C6 product biosynthetic pathway in *C. carboxidivorans* P7 were constructed and putative encoding genes of each enzyme/protein involved in the two pathways were characterized (Fig. 5, Additional file 2: Table S3). Using the FPKMs for normalization, the relative expression level of corresponding genes encoding each enzyme/protein is shown in a heat map of Fig. 5.

In the WL pathway, the first step of the methyl branch was the reduction of CO_2 to formate by formate dehydrogenase (FDH encoded by Ccar_RS18620) (Fernández-Naveira et al. 2017b; Latif et al. 2014). It was suspected to be a rate-limiting enzyme due to quite low expression of its encoding gene. Subsequently, formate was stepwise reduced to methyl group through a series of tetrahydrofolate (THF)- and cobalamin-dependent reactions catalyzed by 10-formyl THF synthase (FTS encoded by Ccar_RS18835), bifunctional methenyl-THF cyclohydrolase/methylene-THF dehydrogenase (MTC/MTD encoded by Ccar_RS18825), methylene-THF reductase (MTR encoded by Ccar_RS18815) and methyl transferase (MeTr encoded by Ccar_RS13140/Ccar_RS15510/Ccar_RS18790), respectively (Fernández-Naveira et al. 2017b; Latif et al. 2014). In the carbonyl branch, the enzyme complex, carbon monoxide dehydrogenase/acetyl-CoA synthase (CODH/ACS, CODH encoded by Ccar_RS07140/Ccar_RS23090 and ACS encoded by Ccar_RS18785/Ccar_RS18795/Ccar_RS18800) reduced CO_2 to CO and then condensed the methyl group and CO into acetyl-CoA, together with coenzyme A (Fernández-Naveira et al. 2017b; Latif et al. 2014). Overall, the expression level of these genes was significantly higher at C37-24 and C37-48 than C25-72 and C25-120. Obviously, the expression of genes involved in the WL pathway preferred 37 °C, which supported fast growth of this strain. At T-72, the expression level of these genes was basically somewhere between that at C37-48 and C25-120, indicating the microbe gradually down-regulated metabolic rates of the WL pathway after the temperature declined.

As shown in Fig. 5, the biosynthetic pathway of butyryl-CoA started from acetyl-CoA, which was

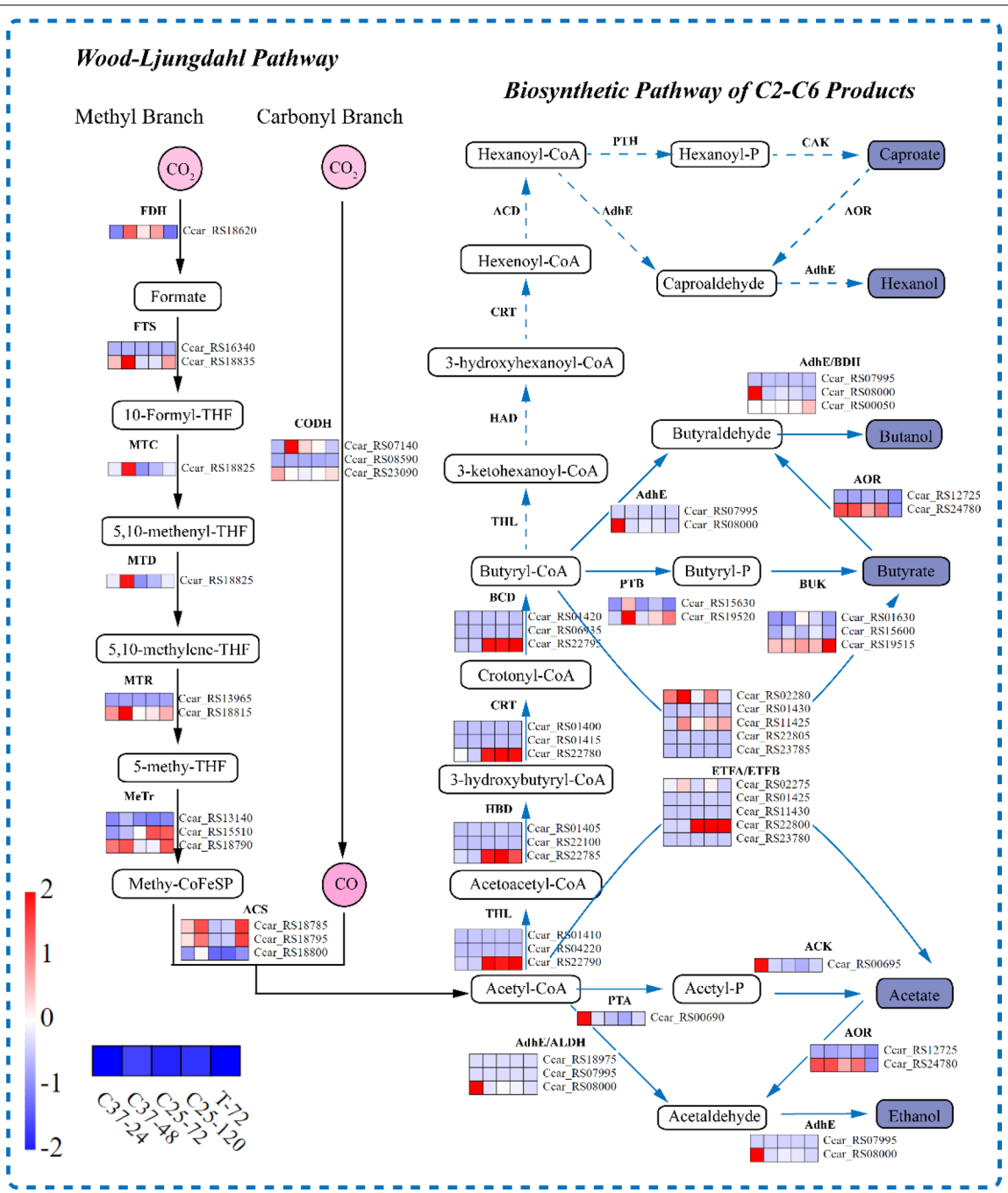

Fig. 5 Schematic diagram of the Wood–Ljungdahl pathway and C2–C6 product biosynthetic pathway in *C. carboxidivorans* P7. Genes' expression level of each enzyme/protein is represented in a heat map using the FPKMs. Each box represents the transcript of one time-point in triplicate. Among the encoding genes of each enzyme/protein, the high-expressed genes are indicated in red, low-expressed ones are indicated in blue, and medium-expressed ones are indicated in white. The full annotations of the corresponding enzymes/proteins and genes are given in Additional file 2: Table S3. The end-products of C2–C6 product biosynthetic pathway are in blue boxes. The solid black arrow indicates the defined reaction of the Wood–Ljungdahl pathway; the solid blue arrow indicates the defined reaction of the C2–C4 product biosynthetic pathway; the dotted blue arrow indicates the putative reaction of the C6 product biosynthetic pathway

subsequently catalyzed by thiolase (THL encoded by Ccar_RS22790), 3-hydroxybutyryl-CoA dehydrogenase (HBD encoded by Ccar_RS22785), crotonase (CRT encoded by Ccar_RS22780) and butyryl-CoA dehydrogenase (BCD encoded by Ccar_RS22795), together with electron transfer flavoprotein α/β (ETFA/B, ETFA encoded by Ccar_RS02280/Ccar_RS11425 and ETFB encoded by Ccar_RS02275/Ccar_RS22800) into butyryl-CoA (Fernández-Naveira et al. 2017b; Ramió-Pujol et al. 2015b). Unexpectedly, the expression of these genes dominated by a gene cluster was more advantageous at 25 °C (C25-72, C25-120, T-72) than 37 °C (C37-24, C37-48). According to the assumption, those enzymes contributed to the formation of hexanoyl-CoA from butyryl-CoA were believed the same enzymes that convert acetyl-CoA into butyryl-CoA (Fernández-Naveira et al. 2017b; Ramió-Pujol et al. 2015b), but it needs further verification with developing molecular tools.

The production of acetate and ethanol predominated in the early culture stage (Fernández-Naveira et al. 2019). The acetyl-CoA was converted to acetate by phosphate acetyltransferase (PTA encoded by Ccar_RS00690) and acetate kinase (ACK encoded by Ccar_RS00695) for the generation of one ATP, which was consumed in the methyl branch (Sun et al. 2019). Meanwhile, acetyl-CoA was catalyzed to ethanol by aldehyde/alcohol dehydrogenase (AdhE encoded by Ccar_RS08000) (Fernández-Naveira et al. 2017b; Ramió-Pujol et al. 2015b). At C37-24, the biomass was increased rapidly with high expression of these three encoding genes. Aldehyde oxidoreductase or aldehyde:ferredoxin oxidoreductase (AOR, encoded by Ccar_RS24780/Ccar_RS12725) was critical for ethanol formation from acetate (Liew et al. 2017; Xie et al. 2015). The genes encoding AOR expressed highly at both 25 °C (C25-72, C25-120) and 37 °C (C37-24, C37-48), verifying the result that acetate accumulated at low concentrations in the culture of any temperature from 25 to 37 °C when using the modified medium that supported high alcohol/acid ratio (Shen et al. 2017). In addition, the encoding gene of butanol dehydrogenase (BDH encoded by Ccar_RS00050) responsible for the generation of butanol was expressed highly at T-72.

These transcripts explained the superiority of the TST culture of 37–25 °C. In the early culture stage, high transcription of the WL pathway at 37 °C facilitated the bacteria to fix carbon for the generation of biomass and C2 products, while in the late culture stage, high transcription of genes associated with acyl-condensation reactions at 25 °C directed carbon and reducing equivalent flow to the formation of C4–C6 products.

Conclusion

In hexanol–butanol–ethanol fermentation by *C. carboxidivorans* P7, higher temperatures (33 and 37 °C) promoted rapid growth but caused cellular agglomeration, and lower temperatures (25 and 29 °C) avoided agglomeration but resulted in slow growth and low production. The TST culture of 37–25 and 37–29 °C could overcome these shortcomings and achieve high higher-alcohol production. Based on anti-agglomerating from Tween 80 or saponin, temperature was proved to play a critical role in higher-alcohol production. The transcriptional analysis revealed high expression of genes in carbon-fixation pathway at 37 °C and product biosynthetic pathway at 25 °C. This study provided two strategies to promote high-density culture, and initially revealed the temperature-effect mechanism on syngas fermentation by *C. carboxidivorans* P7.

Supplementary information

Supplementary information accompanies this paper at https://doi.org/10.1186/s40643-020-00344-4.

Additional file 1. The surfactant-screening experiment, including **Fig. S1.** Growth and production of *C. carboxidivorans* P7 at 37 °C with the addition of different surfactants

Additional file 2: Table S1. Alignment statistic of transcripts. **Table S2.** KEGG pathway enrichment analysis of DEGs. **Table S3**. Expression of genes related to the Wood–Ljungdahl pathway and C2–C6 product biosynthetic pathway.

Abbreviations

C2: Two-carbon chain; C4: Four-carbon chain; C6: Six-carbon chain; WL pathway: Wood–Ljungdahl pathway; CT culture: Constant temperature culture; TST culture: Two-step temperature culture; FPKM: Fragments per kilobase of transcript per million mapped reads; DEG: Differentially expressed gene; SPR: Special production rate; EPS: Extracellular polymeric substance.

Acknowledgements

This study was supported by State Key Laboratory of Bioreactor Engineering, ECUST and CAS-Key Laboratory of Synthetic Biology.

Authors' contributions

SH-S performed the experiments and wrote this paper; G-W and YH-W helped to improve this paper; all authors participated in experiment design and research supervision. All authors read and approved the final manuscript.

Funding

This work was supported by the National Natural Science Foundation of China (31630003), Science and Technology Commission of Shanghai Municipality (17JC1404800), and the Youth Innovation Promotion Association of the Chinese Academy of Sciences (membership 2012213).

Availability of data and materials

All data analyzed during this study are included in this article.

Ethics approval and consent to participate

Not applicable.

Consent for publication

Not applicable.

Competing interests
The authors declare that they have no competing interests.

Author details
[1] State Key Laboratory of Bioreactor Engineering, East China University of Science and Technology, Shanghai 200237, China. [2] Key Laboratory of Synthetic Biology, CAS Center for Excellence in Molecular Plant Sciences, Shanghai Institute of Plant Physiology and Ecology, Chinese Academy of Sciences, Shanghai 200032, China.

Received: 30 June 2020 Accepted: 14 October 2020
Published online: 22 October 2020

References

Drake HL (1982) Demonstration of hydrogenase in extracts of the homoacetate-fermenting bacterium *Clostridium thermoaceticum*. J Bacteriol 150:702–709
Dürre P (2007) Biobutanol: an attractive biofuel. Biotechnol J 2:1525–1534. https://doi.org/10.1002/biot.200700168
Felmann T, Carlile H, Blankenhorn C (1974) Process for dispersing cellular micro-organisms with chelating aqueous alkaline surfactant systems. United States Patent US34623673, 1973-03-29
Fernández-Naveira A, Abubackar HN, Veiga MC, Kennes C (2016) Efficient butanol–ethanol (B–E) production from carbon monoxide fermentation by*Clostridium carboxidivorans*. Appl Microbiol Biotechnol 100:3361–3370. https://doi.org/10.1007/s00253-015-7238-1
Fernández-Naveira Á, Abubackar HN, Veiga MC, Kennes C (2017a) Production of chemicals from C1 gases (CO, CO_2) by *Clostridium carboxidivorans*. World J Microbiol Biotechnol 33:43. https://doi.org/10.1007/s11274-016-2188-z
Fernández-Naveira Á, Veiga MC, Kennes C (2017b) H–B–E (hexanol–butanol–ethanol) fermentation for the production of higher alcohols from syngas/waste gas. J Chem Technol Biotechnol 92:712–731. https://doi.org/10.1002/jctb.5194
Fernández-Naveira Á, Veiga MC, Kennes C (2019) Selective anaerobic fermentation of syngas into either C2–C6 organic acids or ethanol and higher alcohols. Bioresour Technol 280:387–395. https://doi.org/10.1016/j.biortech.2019.02.018
Guan R, Yuan X, Wu Z, Wang H, Jiang L, Li Y, Zeng G (2017) Functionality of surfactants in waste-activated sludge treatment: a review. Sci Total Environ 609:1433. https://doi.org/10.1016/j.scitotenv.2017.07.189
Inoue A, Horikoshi K (1989) A Pseudomonas thrives in high concentrations of toluene. Nature 338:264. https://doi.org/10.1038/338264a0
Latif H, Zeidan AA, Nielsen AT, Zengler K (2014) Trash to treasure: production of biofuels and commodity chemicals via syngas fermenting microorganisms. Curr Opin Biotechnol 27:79–87. https://doi.org/10.1016/j.copbio.2013.12.001
Lee SY, Park JH, Jang SH, Nielsen LK, Kim J, Jung KS (2008) Fermentative butanol production by *Clostridia*. Biotechnol Bioeng 101:209–228. https://doi.org/10.1002/bit.22003
Li B, Dewey CN (2011) RSEM: accurate transcript quantification from RNA-Seq data with or without a reference genome. BMC Bioinform 12:323. https://doi.org/10.1186/1471-2105-12-323
Liew F, Henstra AM, Kpke M, Winzer K, Simpson SD, Minton NP (2017) Metabolic engineering of *Clostridium autoethanogenum* for selective alcohol production. Metab Eng 40:104–114. https://doi.org/10.1016/j.ymben.2017.01.007
Maddox IS, Steiner E, Hirsch S, Wessner S, Gutierrez NA, Gapes JR, Schuster KC (2000) The cause of "acid crash" and "acidogenic fermentations" during the batch acetone–butanol–ethanol (abe-) fermentation process. Microbiol Biotechnol 2:95–100
Molino A, Larocca V, Chianese S, Musmarra D (2018) Biofuels production by biomass gasification: a review. Energies 11:1–31. https://doi.org/10.3390/en11040811
Nielsen PH, Jahn A (1999) Extraction of EPS. In: Jost Wingender T, Flemming H-C (eds) Microbial extracellular polymeric substances. Springer, Berlin, pp 49–72. https://doi.org/10.1007/978-3-642-60147-7
Pantaléon V, Bouttier S, Soavelomandroso AP, Janoir C, Candela T (2014) Biofilms of *Clostridium* species. Anaerobe 30:193–198. https://doi.org/10.1016/j.anaerobe.2014.09.010
Phillips JR, Atiyeh HK, Tanner RS, Torres JR, Saxena J, Wilkins MR, Huhnke RL (2015) Butanol and hexanol production in *Clostridium carboxidivorans* syngas fermentation: medium development and culture techniques. Bioresour Technol 190:114–121. https://doi.org/10.1016/j.biortech.2015.04.043
Price PB, Sowers T (2004) Temperature dependence of metabolic rates for microbial growth, maintenance, and survival. Proc Natl Acad Sci USA 101:4631–4636. https://doi.org/10.1073/pnas.0400522101
Ramachandriya KD, Kundiyana DK, Wilkins MR, Terrill JB, Atiyeh HK, Huhnke RL (2013) Carbon dioxide conversion to fuels and chemicals using a hybrid green process. Appl Energy 112:289–299. https://doi.org/10.1016/j.apenergy.2013.06.017
Ramió-Pujol S, Ganigue R, Baneras L, Colprim J (2015a) Incubation at 25 degrees C prevents acid crash and enhances alcohol production in *Clostridium carboxidivorans* P7. Bioresour Technol 192:296–303. https://doi.org/10.1016/j.biortech.2015.05.077
Ramió-Pujol S, Ganigué R, Bañeras L, Colprim J (2015b) How can alcohol production be improved in carboxydotrophic *clostridia*? Process Biochem 50:1047–1055. https://doi.org/10.1016/j.procbio.2015.03.019
Sardessai Y, Bhosle S (2002) Tolerance of bacteria to organic solvents. Res Microbiol 153:263–268. https://doi.org/10.1016/S0923-2508(02)01319-0
Sen S, Makkar H, Muetzel S, Becker K (1998) Effect of *Quillaja saponaria* saponins and *Yucca schidigera* plant extract on growth of *Escherichia coli*. Lett Appl Microbiol 27:35–38. https://doi.org/10.1046/j.1472-765X.1998.00379.x
Shen S, Gu Y, Chai C, Jiang W, Zhuang Y, Wang Y (2017) Enhanced alcohol titre and ratio in carbon monoxide-rich off-gas fermentation of *Clostridium carboxidivorans* through combination of trace metals optimization with variable-temperature cultivation. Bioresour Technol 239:236–243. https://doi.org/10.1016/j.biortech.2017.04.099
Sheng G-P, Yu H-Q, Li X-Y (2010) Extracellular polymeric substances (EPS) of microbial aggregates in biological wastewater treatment systems: a review. Biotechnol Adv 28:882–894. https://doi.org/10.1016/j.biotechadv.2010.08.001
Sun X, Atiyeh HK, Huhnke RL, Tanner RS (2019) Syngas fermentation process development for production of biofuels and chemicals: a review. Bioresour Technol Rep. https://doi.org/10.1016/j.biteb.2019.100279
Vital-Lopez FG, Reifman J, Wallqvist A (2015) Biofilm formation mechanisms of *Pseudomonas aeruginosa* predicted via genome-scale kinetic models of bacterial metabolism. PLoS Comput Biol. https://doi.org/10.1371/journal.pcbi.1004452
Wainaina S, Horváth IS, Taherzadeh MJ (2018) Biochemicals from food waste and recalcitrant biomass via syngas fermentation: a review. Bioresour Technol 248:113–121
Wang Y, McAllister T, Yanke L, Cheeke P (2000) Effect of steroidal saponin from *Yucca schidigera* extract on ruminal microbes. J Appl Microbiol 88:887–896. https://doi.org/10.1046/j.1365-2672.2000.01054.x
Xie BT, Liu ZY, Tian L, Li FL, Chen XH (2015) Physiological response of *Clostridium ljungdahlii* DSM 13528 of ethanol production under different fermentation conditions. Bioresour Technol 177:302–307. https://doi.org/10.1016/j.biortech.2014.11.101
Yeung C, Thomson M (2013) Experimental and kinetic modeling study of 1-hexanol combustion in an opposed-flow diffusion flame. Proc Combust Inst 34:795–802. https://doi.org/10.1016/j.proci.2012.06.163
Younesi H, Najafpour G, Mohamed AR (2005) Ethanol and acetate production from synthesis gas via fermentation processes using anaerobic bacterium, *Clostridium ljungdahlii*. Biochem Eng J 27:110–119. https://doi.org/10.1016/j.bej.2005.08.015
Zhang J, Taylor S, Wang Y (2016) Effects of end products on fermentation profiles in *Clostridium carboxidivorans* P7 for syngas fermentation. Bioresour Technol 218:1055–1063. https://doi.org/10.1016/j.biortech.2016.07.071

Publisher's Note